

Investigation of properties of laminar antiferromagnetic nanostructures

*B. V. Malozyomov**, Cand. Eng., Associate Prof.¹, e-mail: malozyomov@corp.nstu.ru;

*V. S. Tynchenko**, Cand. Eng., Associate Prof.^{2,3,4}, e-mail: vadimond@mail.ru;

V. A. Kukartsev, Cand. Eng., Associate Prof.³, Polytechnic Institute, e-mail: vkukarstev@sfu-kras.ru;

K. A. Bashmur, Senior Lecturer³, e-mail: bashmur@bk.ru;

T. A. Panfilova, Cand. Eng., Associate Prof.³, e-mail: tpanfilova@sfu-kras.ru

¹ Novosibirsk State Technical University (Novosibirsk, Russia)

² Reshetnev Siberian State University of Science and Technology (Krasnoyarsk, Russia)

³ Siberian Federal University (Krasnoyarsk, Russia)

⁴ Bauman Moscow State Technical University (Moscow, Russia)

* Corresponding authors: B. V. Malozyomov, V. S. Tynchenko.

When creating products using magnetoresistive materials based on magnetic and non-magnetic metals, one is focused on achieving giant magnetoresistance. Such an effect, obtained at the turn of 1980–90-ies years of the last century in superlattices, reached 10–80 % with the intensity of tens of kE at 4.5 K. By methods of physics of magnetic phenomena the regularities of interaction between ferromagnetics and antiferromagnetics, constituting alloys, are determined for strengthening the design of spin valves. Insights into the formation of anisotropy in manganese and permalloy bilayers are detailed. Differences of layer creation causally related to the thermomagnetic activation mode of the process have been determined. The use of alloys in antiferromagnetic nanostructures can indeed lead to the formation of unidirectional anisotropy with changing values of the exchange shift of the hysteresis loop. It has been shown that nanostructures containing alloys exhibit improved magnetism and exchange interaction properties. These results confirm the potential of alloys in creating materials with improved magnetic phenomena and possible applications in various fields such as electronics and magnetic devices.

Key words: antiferromagnetics, nanostructure, magnetoresistive materials, voltage, spin valve, anisotropy, bilayer.

DOI: 10.17580/cisisr.2024.01.13

Introduction

The phenomenon of giant magnetoresistance (GMR) [1, 2] of magnetoresistive materials based on magnetic and nonmagnetic metals ensures their relevance in the production of nanoproducts [3]. GMR is a quantum mechanical effect observed in thin metallic films consisting of alternating ferromagnetic and conducting nonmagnetic layers. The magnetoresistive effect is characterized by a magnitude of 12–75 % large intensity in the saturation field H_s [4]. According to the physical approach to the study of the state of typical antiferromagnetics their transformation into paramagnetics is a phase transition of the second kind. It is characterized not only by the equality of isobaric potentials, but also by the equality of entropies and volumes of phases coexisting in equilibrium, i.e. by the absence of thermal effect of the process and volume change at the transformation temperature. But there are varieties of these substances which realize such transformation at temperatures not reaching the values of the Neel point. In significant magnetic fields the ordered arrangement of atomic spins is partially disturbed. The consequence of this is that the dipole moments of sublattices under their influence “line up” in parallel. The de-

pendence of the magnetization of the investigated substance on the magnitude of the applied external field is determined by the type of a particular structure and the orientation of the field formation relative to the crystal axes. In some samples of antiferromagnetics anomalous behavior is observed in the following parameters Antiferromagnetic alloys find their application in the form of layers for parts of responsible purpose. These can be layers applied to the surface of spin valves. Another application of such alloys is the interaction of ferromagnetics (FM) and antiferromagnetics (AF). For antiferromagnetic alloys, it is a priority to study the regularities of the phenomenon of directional anisotropy. Such anisotropy is formed in the bilayers of such alloys and its study is the most important task.

At the end of the last century, the spin valve [5], which is a nanostructured structure in the form of layered compounds of ferromagnetics and nonferromagnetics [6], was approved. When the magnetic field H_{ex} changes as a result of the interaction of the layers, the magnetic hysteresis curve of the bilayer shifts along the magnetic field axis.

The increase of magnetoresistance by 5–15 % and sensitivity by 1–5 % explains the demand for spin valves in the production of microelectronics products [7]. The prospect

of using spin valves has increased the relevance of the development of antiferromagnetics, so the search for antiferromagnetic materials that create the effect of unidirectional anisotropy requires continuation. In spin valves, the fixing layer is created by using double alloys including manganese, such as FeMn, IrMn, NiMn, PtMn [6].

Alloy Fe₅₀Mn₅₀ is characterized by the ability to create the field of hysteresis loop displacement, but has low corrosion resistance. Alloy Ni₅₀Mn₅₀ is characterized by higher characteristics with the prospect of their improvement by annealing [6].

To improve the performance of layer interaction and is proposed to use alloys Ni–Fe–Mn, in which the disadvantages of previously used alloys are minimized.

Studies [8] confirm that solid solutions under certain conditions exhibit antiferromagnetic properties and can find application in spin valves to anchor the system due to the emergence of antiferromagnetic phase [9]. The regularities and the ability to sustainably obtain the ternary phase have not been sufficiently investigated, which explains the relevance of antiferromagnetic materials for improving the properties of magnetic nanostructures.

The aim of the present work is to investigate the properties of laminar antiferromagnetic nanostructures and to optimize the processing regimes in the process of AF phase preparation.

The set goal is achieved by solving the tasks:

1. Improved properties of FM and AF bilayers with unidirectional anisotropy effect by optimizing processing parameters.
2. Creation of films with antiferromagnetic monolayer by optimizing the composition of components and processing modes.
3. Optimization of parameters for creating manganese/permalloy bilayers for the formation of antiferromagnetic phase.

At processing temperatures above 300 °C, instead of forming an antiferromagnetic phase, decomposition into a manganese and permalloy phase occurs.

The present work details the formation of exchange interaction in nanostructures with antiferromagnetic ternary alloys, establishes the relationship between the structure and properties of nanostructures, and determines the parameters for creating spin valves with improved magnetic and magnetoresistive characteristics.

Research methods and materials

The basis of the research was the detailing of the effect of giant magnetoresistance, which is an order of magnitude higher than the effect of anisotropic magnetoresistance [10, 11].

Samples were produced by electron beam sputtering on a high-vacuum Varian (USA) machine using the MPS-4000-C6 (Ulvac) magnetron sputtering system. The quality of magnetron sputtering was controlled by scanning electron microscope.

We proceeded from the position that the HMS effect manifests itself better when the transformation of neigh-

boring magnetization layers into a parallel structure is observed [12]. The inhomogeneity of the magnetic field and crystal lattice destruction were also taken into account in the experiments [13].

The effect of HMS was evaluated by the criterion of magnetoresistance in the field strength [14–16].

Materials for exchange displacement hysteresis loop

The efficiency of the exchange shift of the hysteresis loop in the layers depends on the interface energy J_{ex} :

$$J_{ex} = H_{ex} \cdot M_{FM} \cdot t_{FM}, \quad (1)$$

where M_{FM} is the saturation of the ferromagnet;

t_{FM} – layer thickness;

H_{ex} – exchange displacement field of the hysteresis loop.

Thin-film structures with the effect of exchange displacement of the hysteresis loop allow controlling the interfaces [17–20]. Ferri/FM, AF/ferri and ferri/ferri ferromagnetics have been investigated as representatives of layered systems. In the present study, the structures of transition metal oxidized transition metal films were investigated Co–CoO, Ni–NiO, Fe–FeO and Ni₈₀Fe₂₀.

Co films are characterized by an increased shift of the hysteresis loop [21], while Ni and Fe films are characterized by a smaller shift [22].

One of the common AF systems is the Fe₅₀Mn₅₀ system [23]. This system has an exchange shift and is among the most studied. The antiferromagnetic Ni_xMn_x [24] has greater corrosion resistance compared to Fe₅₀Mn₅₀ [25]. Nonmetallic systems with exchangeable shear include sulfides, fluorides and nitrides, of which the typical systems are FeS, FeF₂ and MnF₂, as well as the CrN system.

The FM/ferri (Fe₂₀Ni₈₀/TbCo [38], Fe₂₀Ni₈₀DyCo, Ni₈₀Fe₂₀TbFe and Fe/Fe₃O₄) or ferri/AF (Fe₃O₄/CoO and Fe₃O₄/NiO) system are characterized by an increased exchange shift, while the Fe₃O₄·CoO (ferri/AF) system is characterized by the largest shift (2.2 erg/cm²) at 10 K [26].

Spin valves are characterized by increased magnetoresistance (5–15%) and high sensitivity (1–5)/E, which expands the range of their use in production. Most often antiferromagnetics with Neel temperature exceeding room temperature, including manganese, are used. After thermomagnetic treatment the bilayer blocking temperature is 330 °C, which is higher than the Neel temperature.

The authors of the paper investigated permalloy/manganese bilayers. In the course of their studies they showed the conditions of unidirectional anisotropy in these layers. It appears at annealing temperature values of 300 °C [27]. The work is devoted to the study of the same bilayers. In the development of the previous work, the authors showed that annealing allows the formation of an anchoring layer. In this case, the magnetoresistance of such a layer will be 1%. The authors showed that unidirectional anisotropy can occur at annealing with lower temperatures. In their work, the anisotropy occurred at an annealing temperature of 235 °C.

The maximum value of the exchange bias of the hysteresis loop is achieved by a four-hour treatment at 290 °C. The value of the displacement will be 285 E. For permalloy grains, manganese diffusion occurs along their boundaries, resulting in anisotropy with the appearance of AF phase.

In [13, 14], attempts to obtain thin films of composition $(\text{Ni}_{80}\text{Fe}_{20}) \times \text{Mn}_{1x}$ resulted in the stratification of the systems into permalloy and manganese.

Magnetron sputtering of substrates made of single crystal sapphire (1012) Al_2O_3 and glass (Corning) was performed in Aspire 150 machine in magnetic field at argon pressure in the chamber $-(2-4) \times 10^{-7}$ Pa.

The parameters of the used apparatus in the process of coating sputtering: the power of magnetron included in the unit was 125 W; the pressure in the working chamber before filling it with argon was 2.69×10^{-7} Pa; the value of pressure in the working chamber during sputtering was 0.2 Pa; the temperature of substrate heating was 24 ± 3 °C; the value of magnetic field strength was 114 E; the rotation frequency of the substrate during sputtering was 11 rpm; the value of gas purity was 99.8998 %. The results of the study are summarized in the **Table**.

Vacuum sputtering speed		
Spray material	Process speed, nm/min	Process speed, nm/s
Ta	2.83	0.06
$\text{Ni}_{80}\text{Fe}_{20}$	3.35	0.07
$\text{Co}_{90}\text{Fe}_{10}$	2.9	0.06
Cu	7.24	0.12
$(\text{Ni}_{80}\text{Fe}_{20})_{60}\text{Mn}_{40}$	4.14	0.06
$(\text{Ni}_{80}\text{Fe}_{20})_{40}\text{Mn}_{60}$	4.61	0.07
$(\text{Ni}_{70}\text{Fe}_{30})_{30}\text{Mn}_{70}$	4.24	0.82
$(\text{Ni}_{70}\text{Fe}_{30})_{20}\text{Mn}_{80}$	3.92	0.08
$\text{Fe}_{50}\text{Mn}_{50}$	3.72	0.08

Sputtering at a rate of 5–10 nm/min was performed in an Amod machine after annealing the substrate at a temperature regime of 258 °C for a time of 1.5 hours.

The surface of the samples was cleaned by etching in the RITU-VP-1 unit (**Fig. 1**).

The substrate was placed on the electrode. A voltage with a frequency of 14.5 MHz was applied to the electrode. At a temperature of 20 °C during a full technological cycle in argon atmosphere etching of the sample $\text{Al}_2\text{O}_3/\text{Ni}_{77}\text{Fe}_{23}$ (5nm) / Mn (50nm) / $\text{Ni}_{77}\text{Fe}_{23}$ (30nm) / Ta (5nm), annealed at 255 °C for a time of 4 h, at a rate of 1.5 nm/min was performed.

The magnetic characteristics of the films were investigated on a VSM-01 vibrating magnetometer at room temperature, comparing the results obtained with the reference data.

Performance characteristics for the used AVM-1 magnetometer:

- mass of ferromagnetic - 0.5×10^{-6} g – 50 mg.
- sensitivity – 10^{-6} eme;
- magnetic field strength – 0–25 kE;

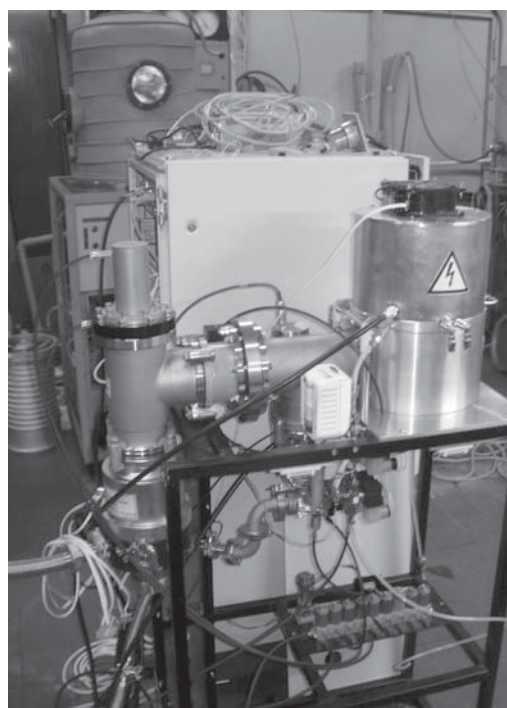


Fig. 1. Installation for ion-plasma etching of experimental samples.

The structure of the compound $(\text{Ni}_{80}\text{Fe}_{20})_{40}\text{Mn}_{60}$ has been investigated in the IWV-2M atomic reactor. It was determined that monochromatic neutrons have a wavelength λ equal to 1.529. The representativeness of the study was increased by using a thermal neutron detector.

Results and discussion

The crystal and magnetic structures were investigated using helium refrigeration. The studies were carried out at temperatures of 4.2–350 K. Quantitative analysis of neutronograms was carried out using the program “Fullprof”. The chemical composition was studied on FEI Inspect F scanning electron microscope with EDAX spectrometer. The composition of the films was found to be identical to that of the target samples by X-ray microanalysis.

The AF fixing layer was created from FeMn and NiMn dual alloys. With fusion $\text{Ni}_{50}\text{Mn}_{50}$ has higher performance, but annealing slightly reduces it.

The efficiency of exchange interaction in Ni–Fe–Mn alloys increases. Thus in the Ni–Fe–Mn system the state of unidirectional anisotropy can be acquired by solid solutions.

Ni–Fe–Mn alloy is in both ferro-, antiferro- and paramagnetic states at room temperature. While the permalloy-manganese alloy $(\text{Ni}_{80}\text{Fe}_{20})_{1-x}\text{Mn}_x$ exists only in the paramagnetic state. For antiferromagnetic ordering, the concentration of manganese must be greater than 0.50 atomic %.

The saturation capacity of M_s of group 1 samples is determined by the amount of exchangeable energy [28].

The hysteresis loops of the samples sputtered on the sapphire substrate are shown in **Fig. 2**.

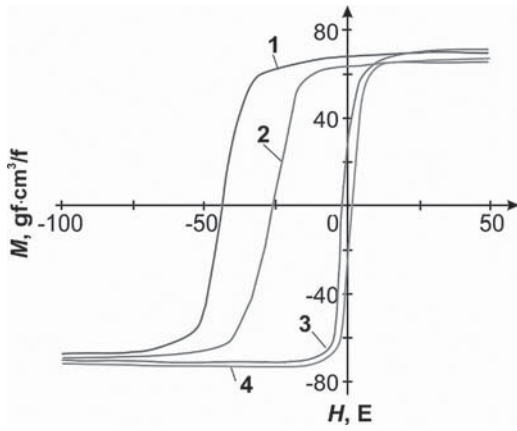


Fig. 2. Hysteresis loops of samples $\text{Al}_2\text{O}_3 / \text{Ta}$ (5 nm) / $\text{Ni}_{80}\text{Fe}_{20}$ (20 nm) / $(\text{Ni}_{80}\text{Fe}_{20})_{40}\text{Mn}_{60}$ (50 nm) / Ta (5 nm) (1) and $\text{Al}_2\text{O}_3 / \text{Ta}$ (5 nm) / $\text{Ni}_{80}\text{Fe}_{20}$ (20 nm) / $(\text{Ni}_{70}\text{Fe}_{30})_{30}\text{Mn}_{70}$ (50 nm) / Ta (5 nm) (2)

Unidirectional anisotropy does not occur if the blocking temperature of the bilayer is less than room temperature. Influence The thickness of the AF layer $(\text{Ni}_{70}\text{Fe}_{30})_{30}\text{Mn}_{70}$ significantly affects the bilayer properties. This influence was investigated using samples having a constant thickness permalloy layer. The thickness of the layer was 10 nm. The antiferromagnetic layer had a variable thickness. The thickness of this antiferromagnetic layer varied already in quite significant ranges, from 5 to 80 nm (Fig. 3).

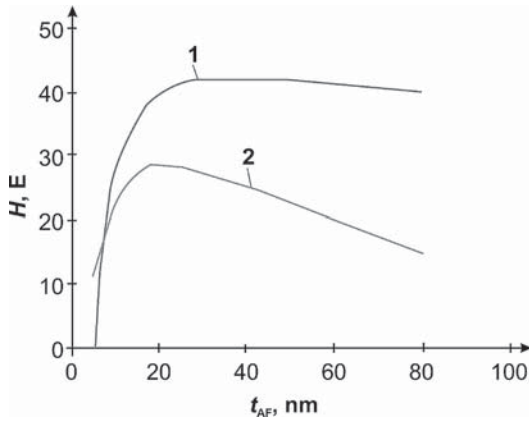


Fig. 3. Dependences of H_{ex} (1) and H_c (2) of $\text{Al}_2\text{O}_3 / \text{Ta}$ (5 nm) / NiFe (10 nm) / $(\text{Ni}_{70}\text{Fe}_{30})_{30}\text{Mn}_{70}$ (t_{AF}) / Ta (5 nm) nanostructures on antiferromagnetic layer thickness, t_{AF}

The results of the study have convergence with the data obtained in the study. Similarly to this study, the required thickness of the saturated layer is shown. The value of its thickness should be 20 nm.

It can be seen from the source [29] that as the thickness of the antiferromagnetic layer increases, the fraction of grains affecting the exchange shear increases. Meiklejohn and Bean describe the exchange shift by the expression:

$$K_{\text{AF}} \cdot t_{\text{AF}} > J_{\text{ex}},$$

where K_{AF} is the AF anisotropy constant;
 t_{AF} – AF thickness.

The grain size distribution [30] is corrected by utilizing the thermal activation capabilities [31, 32]. At low activity of an antiferromagnetic, its grains are in the superparamagnetic state with zero H_{ex} and weak coercivity, and at high activity the energy barrier increases.

Plots of dependence of the values of the parameters H_{ex} and the ferromagnetic layer thick-ness parameter (t_{NiFe}) for samples at $t_{\text{NiFe}} = 5, 15, 20$ nm can be seen from Fig. 4.

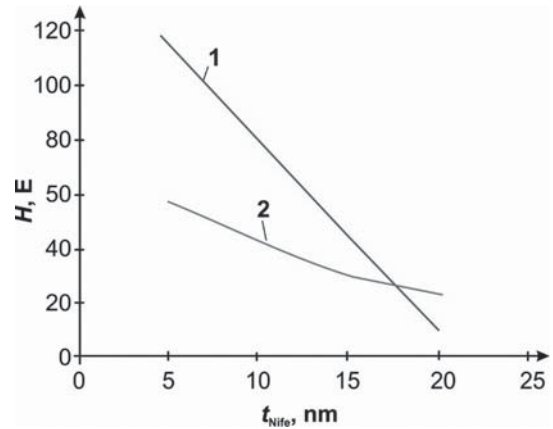


Fig. 4. Dependences of H_{ex} (1) and H_c (2) samples glass / Ta (5 nm) / $\text{Ni}_{80}\text{Fe}_{20}$ (t_{NiFe}) / $(\text{Ni}_{70}\text{Fe}_{30})_{30}\text{Mn}_{70}$ (10 nm) / Ta (5 nm) on permalloy thickness, t_{NiFe}

When the permalloy thickness increases in the range of 5–20 nm, H_{ex} decreases in the range of 120–8.5 E, which confirms the correctness of the statement about the beginning of unidirectional anisotropy from the interfaces.

The graphs H_{ex}, H_c in the nanostructure $\text{Ni}_{80}\text{Fe}_{20} / (\text{Ni}_{70}\text{Fe}_{30})_{30}\text{Mn}_{70}$ (from the thickness of layers confirm the correctness of the conclusions of the authors of [13, 15] (Fig. 5).

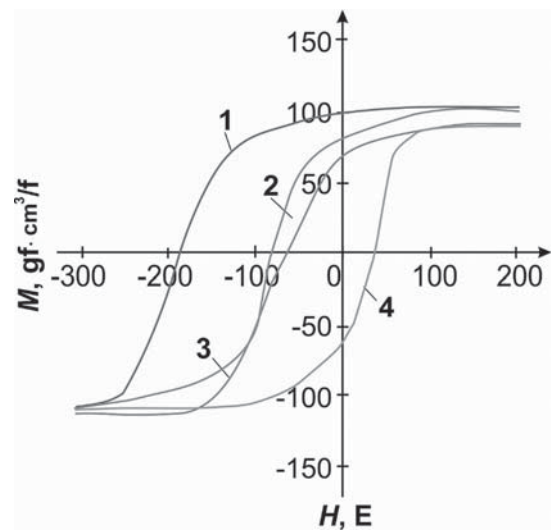


Fig. 5. Magnetic hysteresis loops of samples of Ta (5 nm) / $\text{Ni}_{80}\text{Fe}_{20}$ (5 nm) / $(\text{Ni}_{70}\text{Fe}_{30})_{30}\text{Mn}_{70}$ (10 nm) / Ta (5 nm) prepared on glass (1) and sapphire (2) substrates

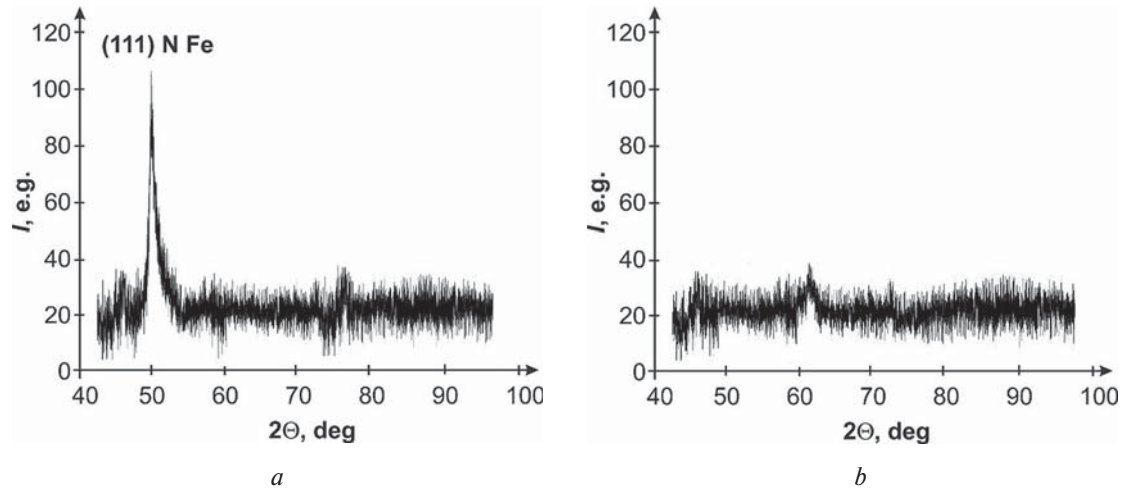


Fig. 6. Diffractograms of samples of Ta (5 nm) / Ni₈₀Fe₂₀ (5 nm) / (Ni₇₀Fe₃₀)₃₀Mn₇₀ (10 nm) / Ta (5 nm) sprayed on sapphire (a) and glass (b) substrates

The hysteresis loops are characterized by high coercivity numerically equal to 55–58 E for sapphire and glass samples, respectively.

X-ray diffraction studies of glass samples revealed an axial texture <111>. The common structural peak for (111) Ni–Fe–Mn and for (111) NiFe can be seen in Fig. 6.

For the occurrence of texture <111> and larger H_{ex} it is reasonable to use glass substrates with minimal roughness. Parameters of thermomagnetic treatment of nanostructures are investigated on a sample of glass / Ta (2 nm) / Ni₈₀Fe₂₀ (5 nm) (Ni₇₀Fe₃₀)₃₀Mn₇₀ (10 nm) / Co₉₀Fe₁₀ (5 nm) / Ta (5 nm). Exchangeable shear occurs only when a buffer layer is created.

The hysteresis loops are shown in Fig. 7. The hysteresis loop displacement parameters are related to the positioning of ferromagnetic and antiferromagnetic layers. In this case, the value of the hysteresis loop shift H_{ex} is larger for the FM/AF layer than for the AF/FM layer.

The hysteresis loop shift parameters in its lower part are comparable to their value for the glass structure / Ta (5 nm) / Ni₈₀Fe₂₀ (5 nm) (Ni₇₀Fe₃₀)₃₀Mn₇₀ (10 nm) / Ta (5 nm).

Crosses highlight the centers of hysteresis loops, which can be used to obtain quantitative values of H_{ex} and H_c for CoFe and NiFe layers.

The close values of H_{ex} and H_c for the interfaces are attributed to the transformation of the double hysteresis loop into a single symmetric loop due to the temperature rise in the magnetic field at 210 °C in a time of 1 hr.

Analysis of the obtained data on volumetric diffusion shows that at the investigated heat treatment regime manganese diffusion is not carried out due to the magnetization stability acquired during annealing.

The shear growth in the structure of Ni₈₀Fe₂₀ / (Ni₇₀Fe₃₀)₃₀Mn₇₀ / Co₉₀Fe₁₀ after heat treatment promotes the formation of <111> texture as a result of reorientation of magnetic phenomena at the layer interface.

The correlation between the AF layer type and the H_{ex} hysteresis loop displacement field is explained in Fig. 8, where the H_{ex} plots of samples of different compositions are compared, which shows that it varies within 145–170 °C.

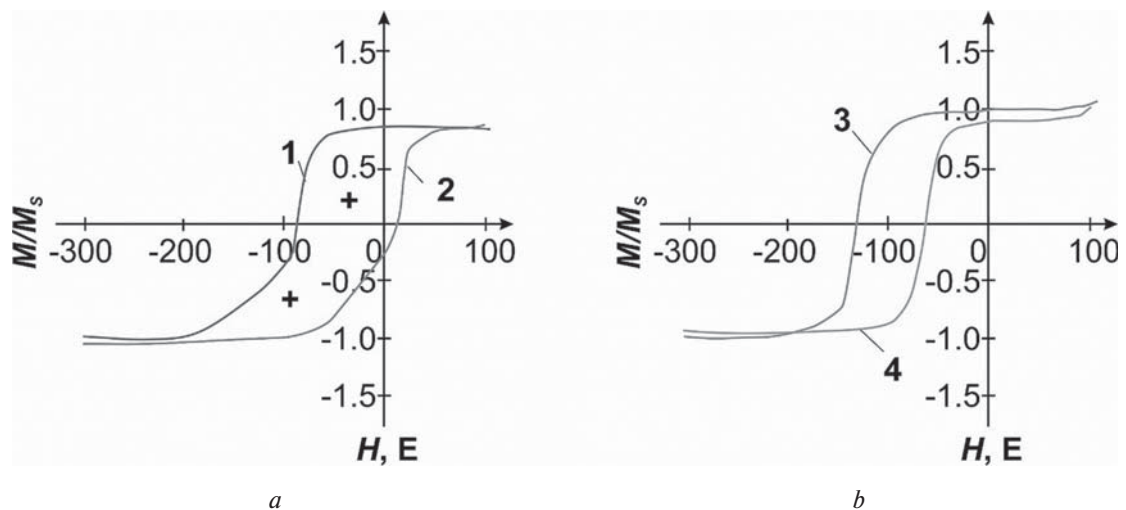


Fig. 7. Magnetic hysteresis loops of samples of glass / Ta (2 nm) / Ni₈₀Fe₂₀ (5 nm) / (Ni₇₀Fe₃₀)₃₀Mn₇₀ (10 nm) / Co₉₀Fe₁₀ (5 nm) / Ta (5 nm): after sputtering (a), after annealing at 200 °C, 1 h (b). The crosses denote the centers of partial hysteresis loops from which the H_{ex} and H_c values were obtained for CoFe and NiFe layers.

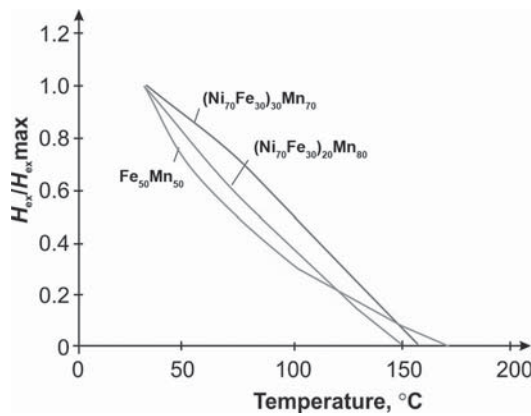


Fig. 8. Dependence of H_{ex} on temperature for different types of AF.

The blocking temperature in samples from compound Ni–Fe–Mn increases with increasing manganese concentration. It is less than the maximum Neel temperature $T_N = 235^\circ\text{C}$ for compound Ni–Fe–Mn of the same composition.

Thus for thin film systems, the size of the film layer determines the blocking temperature, grain size, and the Neel temperature.

It was determined that at a temperature of about 180°C the blocking is possessed by the sample with the AF of the alloy $(\text{Ni}_{70}\text{Fe}_{30})_{20}\text{Mn}_{80}$. Thus, this temperature should be considered as the maximum temperature for blocking of alloys Ni–Fe–Mn.

It is found that the magnitude of the hysteresis loop displacement field and coercive force are subject to adjustment by changing the substrate type, layer thickness and magnetic processing temperature.


Conclusions

1. Unidirectional anisotropy in the FM/AF structure, which contains AF ternary alloy Ni–Fe–Mn, results from their exchange interaction.

2. Magnetic hysteresis curve of the AF layer in nanostructures $\text{Ni}_{80}\text{Fe}_{20} / (\text{Ni}_{70}\text{Fe}_{30})_{30}\text{Mn}_{70}$ is formed when the layer thickness size is larger than 6 nm.

3. For the alloy $(\text{Ni}_{70}\text{Fe}_{30})_{20}\text{Mn}_{80}$ with AF layer, a temperature $t_{\max} = 180^\circ\text{C}$ can be observed under certain conditions. This temperature is observed at the thickness of the AF layer $t_{AF} = 20$ nm, manganese fraction (x_{Mn}) up to 81 atomic %.

4. The use of glass as a substrate material makes it possible to significantly increase H_{ex} in the formation of nanostructured compounds of FM and AF. The use of glass makes it possible to increase H_{ex} by six times compared to the sapphire substrate.

5. Spin valves after magnetic and thermal treatment of the layered structure and hysteresis characteristic shift with a value of H_c / H_{ex} , is of interest to manufacturers. 

REFERENCES

- Seredkin V. A., Iskhakov R. S., Yakovchuk V. Y., Stolyar S. V., Myagkov V. G. Unidirectional anisotropy in film systems (RE–TM) / NiFe. *Fizika tverdogo tela*. 2003. Vol. 45., Iss. 5. pp. 927–931. DOI: 10.1134/1.1575337.
- Ramermann D., Becker A., Bükler B., Hütten A., Ennen I. Nano Scaled Checkerboards: A Long Range Ordering in NiCoMnAl Magnetic Shape Memory Alloy Thin Films with Martensitic Intercalations. *Appl. Sci.* 2022. Vol. 12. p. 1748. DOI: 10.3390/app12031748.
- Becker A., Ramermann D., Ennen I., Bükler B., Matalla-Wagner T., Gottschalk M., Hütten A. The influence of Martensitic Intercalations in Magnetic Shape Memory Ni–Co–Mn–Al *Multi-layered Films*. *Entropy*. 2021. Vol. 23. p. 462.
- Pankratov N. Y., Nikitin S. A., Mitsiuk V. I., Ryzhkovskii V. M. Direct measurement of the magnetocaloric effect in mznnsb intermetallic compound. *Journal of Magnetism and Magnetic Materials*. 2019. Vol. 470. pp. 46–49.
- Coehoorn R. Giant Magnetoresistance and Magnetic Interactions in Exchange-Biased SpinValves. In: K.H.J. Buschow (Ed.), *Handbook of magnetic materials*. Vol. 15. Elsevier B.V.: Amsterdam, 2003. pp. 1–199.
- Freitas P. P., Ferreira R., Cardoso S., Cardoso F. Magnetoresistive sensors. *J. Phys.: Condens. Matt.* 2007. Vol. 19 (16). 165221-1-21.
- Chappert C., Fert A., Nguyen Van Dau F. The emergence of spin electronics in data storage. *Nature Materials*. 2007. No. 6. pp. 813–823.
- Grünberg P. Layered magnetic structures in research and applications. *Acta Mater.* 2000. Vol. 48. pp. 239–251.
- Ovchenkova I. A., Tereshina I. S., Bogdanov A. E., Nikitin S. A., Tereshina-Chitrova E. A., Paukov M. A., Gorbunov D. I. The tremendous influence of hydrogenation on magnetism of NdMnGe. *Intermetallics*. 2019. Vol. 115. p. 106619.
- Li T. Giant magnetoresistance effect in Ni buffered Co/Cu/Co sandwich. *Science in China (Series E)*. 2002. Vol. 45 (2). pp. 166–174.
- Yelemessov K., Sabirova L. B., Bakhmagambetova G. B., Atanova O. V. Modeling and Model Verification of the Stress-Strain State of Reinforced Polymer Concrete. *Materials*. 2023. Vol. 16. 3494. DOI: 10.3390/ma16093494.
- Moran T. J., Gallego J. M., Schuller I. K. Increased exchange anisotropy due to disorder at permalloy/CoO interfaces. *J. Appl. Phys.* 1995. Vol. 78 (3). pp. 1887–1891.
- Isametova M. E., Nussipal R., Efremenkova E. A., Isametov A. Mathematical Modeling of the Reliability of Polymer Composite Materials. *Mathematics*. 2022. Vol. 10. p. 3978. DOI: 10.3390/math10213978.
- Jungblut R., Coehoorn R., Johnson M. T.; Aan de Stegge J., Reinders A. Orientational dependence of the exchange biasing in molecular beam epitaxy grown $\text{Ni}_{80}\text{Fe}_{20} / \text{Fe}_{50}\text{Mn}_{50}$ bilayers. *J. Appl. Phys.* 1994. Vol. 75 (10). pp. 6659–6664.
- Sorokova S. N., Efremenkova E. A., Qi M. Mathematical Modeling of Mechanical Forces and Power Balance in Electromechanical Energy Converter. *Mathematics*. 2023. No. 11. 2394. DOI: 10.3390/math11102394.
- Zheng R. K., Liu H., Zhang X. X., Roy V. A. L., Djuricic A. B. Exchange bias and the origin of magnetism in Mn-doped ZnO tetrapods. *Appl. Phys. Lett.* 2004. Vol. 85 (13). pp. 2589–2591.
- Eid K. F., Stone M. B., Ku K. C. Maksimov O., Schiffer P., Samarth N., Shih T. C., Palmstrom C. J. Exchange biasing of the ferromagnetic semiconductor $\text{Ga}_{1-x}\text{Mn}_x\text{As}$. *Appl. Phys. Lett.* 2004., Vol. 85 (9). pp. 1556–1558.
- Lin H. T., Chen Y. F., Huang P. W., Wang S. H., Huang J. H., Lai C. H., Lee W. N., Chin T. S. Enhancement of exchange coupling between Ga–Mn–As and Ir–Mn with self-organized Mn(Ga)As at the interface. *Appl. Phys. Lett.* 2006. Vol. 89 (26). pp. 262502–262503.
- Huang P.-H., Huang H.-H., Lai C.-H. Coexistence of exchange-bias fields and vertical magnetization shifts in ZnCoO/NiO system. *Appl. Phys. Lett.* 2007. Vol. 90 (6). 062509-3.
- Saren A., Smith A. R., Ullakko K. Integratable magnetic shape memory micropump for high-pressure, precision microfluidic applications. *Microfluid. Nanofluid.* 2018. Vol. 22. p. 38.

21. Sharrock M. P. Recent advances in metal particulate recording media: toward the ultimate particle. *IEEE Trans. Magn.* 2000. Vol. 36 (5). pp. 2420–2425.
22. Sort J., Nogués J., Amils X., Suriñach S., Muñoz J. S. Baró M. D. Room-temperature coercivity enhancement in mechanically alloyed antiferromagnetic-ferromagnetic powders. *Appl. Phys. Lett.* 1999. Vol. 75 (20). pp. 3177–3179.
23. Barbic M., Scherer A. Magnetic nanostructures as amplifiers of transverse fields in magnetic resonance. *Solid State Nucl. Magn. Reson.* 2005. Vol. 28 (2–4). pp. 91–105.
24. Matsuzono A., Terada S., Ono H., Furukawa A. Sone T., Sasaki S., Kakihara Y., Takeda Y., Chiyokubo N. Matsuki H. Study on requirements for shielded current perpendicular to the plane spin valve heads based on dynamic read tests. *J. Appl. Phys.* 2002. Vol. 91 (10). pp. 7267–7269.
25. Kondratiev V. V., Klyuev R. V., Karlina A. I. Improvement of Hybrid Electrode Material Synthesis for Energy Accumulators Based on Carbon Nanotubes and Porous Structures. *Micromachines*. 2023. Vol. 14. p. 1288. DOI: 10.3390/mi14071288.
26. Gallagher W. J., Parkin S. S. P. Development of the magnetic tunnel junction MRAM at IBM: From first junctions to a 16-Mb MRAM demonstrator chip. *IBM J. Res. & Dev.* 2006. Vol. 50 (1). pp. 5–23.
27. Parkin S., Jiang X., Kaiser C., Panchula A., Roche K., Samant M. Magnetically engineered spintronic sensors and memory. *Proceeding of the IEEE 2003*. 2003. Vol. 91 (5). pp. 661–680.
28. Dieny B., Gurney B. A., Lambert S. E., Mauri D., Parkin S. S. P., Speriosu V. S., Wilhoit D. R. Magnetoresistive sensor based on the spin valve effect. U.S. Pat. 5206590 USA. Published. 27.04.93.
29. Malozyomov B. V., Martyushev N. V., Kukartsev V. V., Tynchenko V. S., Bukhtoyarov V. V., Wu X., Tynchenko Y. A., Kukartsev V. A. Overview of Methods for Enhanced Oil Recovery from Conventional and Unconventional Reservoirs. *Energies*. 2023. Vol. 16. 4907. DOI: 10.3390/en16134907.
30. Baumgart P. M., Dieny B., Gurney A., Nozieres J. P., Speriosu V. S., Wilhoit D. R. Dual spin valve magnetoresistive sensor. U.S. Pat. 5287238 USA. Published 15.02.94.
31. Martyushev N. V., Sorokova S. N., Efremenkov E. A., Valuev D. V., Qi M. Analysis of a Predictive Mathematical Model of Weather Changes Based on Neural Networks. *Mathematics*. 2024. Vol. 12. p. 480. DOI: 10.3390/math12030480.
32. Radu F. Zabel H. Magnetic Heterostructures: Advances and Perspectives in Spinstructures and Spintransport. *Series: Springer Tracts in Modern Physics*. Vol. 227. Springer-Verlag: Berlin, 2008. pp. 97–184.
33. Shishkin P. V., Malozyomov B. V., Martyushev N. V., Sorokova S. N., Efremenkov E. A., Valuev D. V., Qi M. Mathematical Logic Model for Analysing the Controllability of Mining Equipment. *Mathematics*, 2024. Vol. 12. p. 1660. DOI: 10.3390/math12111660.